ENGINEERING INTEGRITY, VOLUME 25, SEPTEMBER 2008. pp15-22. ISSN 1365-4101/2008

Technical paper

Deformation and rupture of stainless steel under cyclic, torsional creep

D. W. A. Rees, School of Engineering and Design, Brunel University, Uxbridge, Middlesex, UB8 3PH

Abstract

Recent results from a long-term, strain-limited, cyclic creep test program upon stainless steel tubes are given. The test conditions employed were: constant temperature 500 °C, shear stress $\tau = \pm 300$ MPa and shear strain limits $\gamma = \pm 4$ %. It is believed that a cyclic creep behaviour for the material has been revealed that has not been reported before in the literature. That is, the creep curves for stainless steel under repeated, shear stress reversals shows two basic square root dependencies; one upon time and the other upon cycle number. Consequently, the combined effect is such that the shear creep strain depends upon the square root of the product of cycle number and the time elapsed within that cycle. Despite extended times of cycling, with the test running into a period of over a year, no secondary or tertiary creep stages were ever observed within individual creep curves. Thus both the forward and reversed creep curves were exclusively primary in nature, within which the only visible evidence of a slow degradation of the deforming material was that the creep interval reduced successively between the imposed strain limits. However, it was found that the creep curve, when plotted within axes of cumulative creep strain and time, did recover a "pseudo-tertiary" stage. This stage concords with earlier results that showed tertiary creep to be a dominant contributor to the creep curve for this material under a steady torque [1]. Given either the tensile ductility of the material or, a tensile creep rupture time, it is shown how final failure is predicted from the phenomenological square root law and an equivalence criterion.

Keywords: creep-fatigue interaction, life prediction, creep ductility, cyclic loading, strain control, torsion.

1. Introduction

There are many empirical formulae available to describe each or all stages of the "constant load" creep curve [2]. The time-dependence of the monotonic creep strain has been expressed variously in parabolic, logarithmic, hyperbolic and exponential forms [3]. The latter is often employed to represent the gradual attainment of a steady rate following primary creep, within the following three-part formula:

$$\varepsilon = \varepsilon_o + \varepsilon_p (1 - e^{-m t}) + \dot{\varepsilon}_s t \qquad (1)$$

where t is elapsed time following an instantaneous elastic strain response to the stress applied i.e. $\varepsilon_o = \sigma/E$. The second and third terms are the contributions to total strain ε from primary and secondary creep. Within these terms $\dot{\varepsilon}$ is the observed secondary creep rate and m and ε_p are constants expressing an exponential decay in the primary creep strain. Equation (1) appears to have been first adopted, exclusively for metals, by McVetty [4]. It was also employed by Garofalo [5] and Andrade [6] in the early 1960's for describing creep in 316 stainless steel and cadmium respectively. Latterly, the basic form of eq (1) re-appeared within various predictions to creep strain and rupture time for engineering alloys used in service when times run into years. Here, a further exponential term is added to eq (1) to allow for the period of accelerating strain rates in the tertiary regime prior to failure. Wilshire et al [7, 8] have used the following sums of terms for the instantaneous, primary, secondary and tertiary strains respectively, in their descriptions of the full creep curve for copper alloys:

$$\varepsilon = \varepsilon_o + \varepsilon_p (1 - e^{-m t}) + \dot{\varepsilon}_s t + \varepsilon_L e^{p(t-t_t)} \qquad (2a,b)$$

$$\varepsilon = \varepsilon_o + \varepsilon_p (1 - e^{-m t}) + \dot{\varepsilon}_s t + \varepsilon_L (e^{pt} - 1)$$

where ε_p and m are primary constants, $\dot{\varepsilon}$ is the secondary creep rate and t_t is the time to the start of a tertiary region, within which p and ε_L are constants. Alternatively, where for ferritic steels, the creep curve showed an inflexion from primary to tertiary (without a prolonged region of secondary), these authors [9, 10] proposed their θ - projection concept:

$$\varepsilon = \varepsilon_o + \theta_1 (1 - e^{-\theta_2 t}) + \theta_3 (e^{\theta_4 t} - 1) \qquad (3)$$

where θ_i (i = 1, 2, 3) allow the fit to long term creep curves in this category with good precision. Much less work has been done on the cyclic creep (CC) behaviour of these materials, a condition which may equally well apply to service loading. The various predictive techniques for CC are concerned more with the fracture event than in following the precise nature of the deformation that precedes it. For example, one prediction of the cyclic life N under CC employs only the range of creep strain, in a similar form to that used by Coffin for predicting the low cycle fatigue life N_f [11]. Another prediction relates the accumulated time $\Sigma(\Delta t)$ to rupture to the known creep life t_r under the steady (dwell) stress [12]. If the creep and fatigue processes have interacted, their

respective life fractions are summed by Taira's rule [13] as follows:

$$N / N_f + \Sigma(\Delta t) / t_f = L \qquad (4)$$

where, respectively, N_f and t_f apply to the inelastic strain range (loop width) and the dwell stress in CC and L is a constant, originally taken as unity. Design codes admit L as an empirical constant, different from unity, to allow a more flexible life prediction.

Another approach, to be developed here, is to base the fracture event solely upon the exhaustion of a material's creep ductility [14], in a similar manner to the life fraction summation term in eq(4). That is:

$$\Sigma[(\Delta \varepsilon_c) / \varepsilon_f] = D \qquad (5)$$

where D may reflect the difference between the monotonic creep rupture ductility ε_f and its cyclic creep ductility. Here, under torsion, we find that the latter is greater than the former in a ratio $D \approx 2$. To apply eqs (4) and (5), it is necessary to represent the creep strain curve within each interval accurately. Given, that during each dwell, the material deformed in primary creep, it was found to be accurate to adopt a power law description of the diminishing rates observed. Correspondingly, the creep curve is given as:

$$\gamma = \gamma_o + at^m \qquad (6)$$

where $\gamma_o = \tau/G$ is the instantaneous elastic strain in which G is the shear modulus. The power law, which has had a universal appeal for simple tensile and torsional creep, was proposed originally for non metals [15]. For metals specifically, $m = 1/3$ within the Andrade [16] and Graham-Walles [17] laws; this fractional exponent value being shown, for example, to apply to polycrystalline aluminium and copper [18] and to a binary copper-silver alloy [19]. More generally, for both metal single crystals [20] and polycrystals [21 - 24], m has taken values from 0.2 - 0.7, these descriptions of primary creep having being associated with hardening through an increase in dislocation density [25].

The power law description of "parabolic" or "transient" (i.e. primary) creep has hardly been employed in the far fewer cyclic creep studies, reviewed in [26], and in other cyclic studies concerned with life prediction [27] and damage accumulation [28, 29]. It has been used by the present author in earlier accelerated CC tests upon an austenitic stainless steel [30, 31] at 600°C. There m appeared to be independent of the strain range and dwell stress. In the present study, the dependence of the time exponent $0 < m < 1$ and the coefficient a in eq(6) upon cycle number n are to be investigated over longer creep intervals at a lower temperature (500°C). A known dependence of both a and m upon n will allow the creep strain to be summed to a pre-determined limit, thereby predicting a CC life.

2. Test Procedure

The NPL machine used for this investigation was designed by the NPL and manufactured by W.H. Mayes Ltd. Torsion was applied to a tubular testpiece with cylindrical gauge dimensions: 8.0 mm o.d., 6.4 mm i.d. within a 16 mm length. Beyond this length a 20 mm radius enlarged the o.d. to meet the 10 mm outer square-section ends. The 20 mm end lengths allow their bolted connection to 35 mm diameter nimonic torque bars that supported the testpiece vertically in the centre of a furnace that allowed independent control of its three windings. A platinum-rhodium thermocouple recorded that the temperature was held constant at 500 ± 2°C by compensating for a greater heat loss from the ends with this controller. The upper twist rod was anchored above the furnace and the lower rod was integral with a protractor-pulley that rotated under tangential forces applied through wire lying within its grooved rim. The balanced CC cycle was achieved by allowing a limiting twist in one direction under a single tangential force applied through a constant, hanging dead weight. The twist direction was reversed by applying an opposing tangential force through a second hanging weight of twice the magnitude to reach an equal negative twist. The reversals were imposed by raising and lowering the greater weight from its rest position upon a load cell with a motor-driven screw jack, activated at the two pre-set twist limits. The latter were preset with a rotary transducer whose spindle rotated with the lower twist rod. Both load and twist were plotted together and independently with time throughout the test. Notwithstanding power cuts de-activating the relay circuit, the test was fully automated. It has been noted previously that in this "soft" machine the twist rods themselves wind-up elastically in transmitting torque to the testpiece. The wind-up and the twist in the testpiece were recorded at a remote transducer position, away from the heat zone. Consequently, each twist component contributes to the strain limits set on this transducer. As the twist from the rods is instantaneously elastic and that from the testpiece is time-dependent, the creep strain is easily separated. However, the rod twist does confuse the experimental determination of the smaller amount of the testpiece's instantaneous twist, γ_o in eq (6), which is elastic-plastic. Where the elastic contribution is required it will be found from the shear modulus G as $\gamma_o = \tau/G$, in which τ is the peak (dwell) shear stress. That twist in the solid 25 mm diameter nimonic rods remained elastic and was thus recoverable could be seen from the return to the initial zero setting upon the protractor scale with the insertion of each new testpiece. The creep strain referred to here (e.g. $\Delta\gamma_c$ in Fig.1) has removed all the instantaneous strain, including that which occurs in the rods and the testpiece.

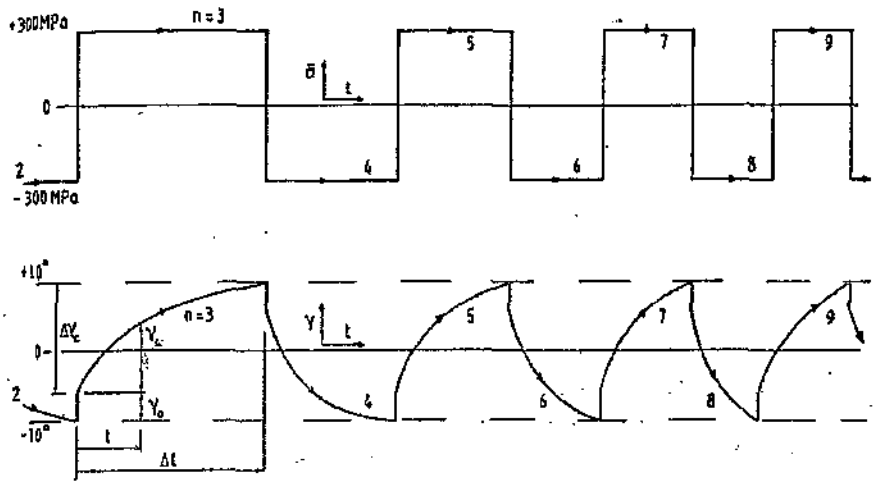

Figure 1 Sample of strain-limited, cyclic torsional creep recordings from $n = 3$ to $n = 9$; (a) shear stress τ versus time t, showing abrupt reversals and (b) shear strain versus time, in which cycle parameters are, instantaneous strain γ_o, creep strain γ_c, dwell creep strain $\Delta\gamma_c$ and time Δt.

Consequently, in common with previous studies [30 - 33], the analysis of γ_o that follows refers to the true, time-dependent, component of strain (creep) within the testpiece.

3. Results

Figures 1a,b show a portion of the continuous time-based recordings (from cycle 3 to cycle 9). The ramped load applications (see Fig. 1a) occur at times when the pre-set strain limits are reached. The shear stress acting during the periods of dwell is calculated from load according to the elastic torsion theory:

$$\tau = T r_m / J = [(WR)(d_o + d_i)/4] / [\pi (d_o^4 - d_i^4)/32] = C_1 W \quad (7a)$$

where W is the smaller tangential load, R is the pulley radius, d_i and d_o are the inner and outer testpiece diameters. These give C_1 = 2.56 in eq(7a) and, with a load W = 67.65 N in eq(7a), the mean shear stress in the wall of the testpiece was ital τ_m = 173.2 MPa (σ = 300 MPa).

The mean shear creep strain is calculated from the transducer twist in radian and degrees measures according to:

$$\gamma_c = [r_m (\theta^c - \theta_o^c)] / l = [\pi (d_i + d_o)(\theta^o - \theta_o^o)] / (4\, l \times 180)$$

$$= C_2 (\theta^o - \theta_o^o) \quad (7b)$$

where θ_o is the wind-up twist that appears at time $t = 0$ in the recording, i.e. the vertical lines in Fig. 1b. This figure shows the notation for a period of creep dwell under τ_m. Given the twist limits $\theta = \pm$ 10°, with C_2 = 3.927 x 10^{-3} in eq (7b), the creep curve is partitioned to provide γ_c at time t and $\Delta\gamma_c$ for each completed interval time Δt. The sample trace shows a successive reduction in Δt with increasing cycle number n. Such a trend was found to be most prevalent for the first 20 reversals, as shown in Fig. 2. Thereafter, the time shortening becomes more gradual, oscillating only slightly between the forward and reverse directions. Despite the trend being marred by a power cut on two occasions, where strain limits over-ran, they were soon restored and with continued, corrected cycling, the data re-aligned with an apparent steady state giving $\Delta t \approx$ 170 h between cycles 30 and 40.

Within the torque-twist plot (see Fig. 3) the diminution in the time interval appears as a rounding of the loops with successive cycling. That is, an increasing plastic component of strain precedes creep, so raising the contribution from instantaneous strain γ_o to the total strain. A failure occurred for n = 47, where, in failing to hold the load in dwell, the reversal involved only rapid plasticity. In the first application of the load (n = 1), the strain range is one half of those strain ranges for the subsequent reversals. In fact, the strain-time response for n = 1, presents the usual features of a monotonic creep response for the material. Depending upon the duration for n = 1, useful primary and, possibly, secondary creep properties may be derived to assist with the life prediction.

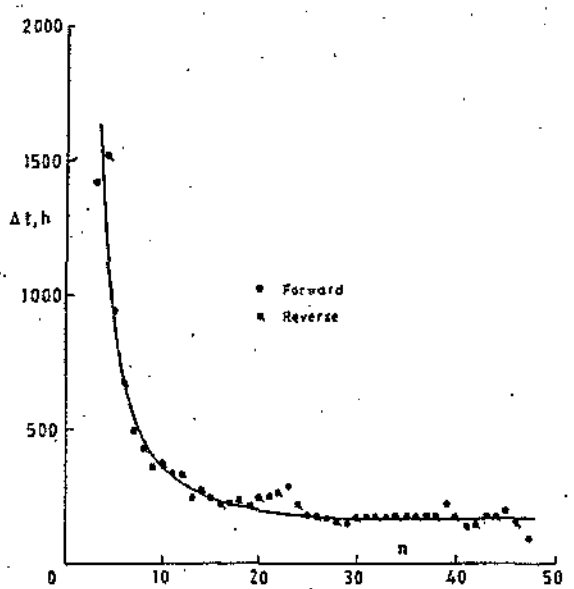

Figure 2 Diminishing dwell time Δt with cycle number n, obeying an approximate hyperbolic relationship $\Delta t \sim 1/n$. Irregularities due only to experimental effects (power cuts).

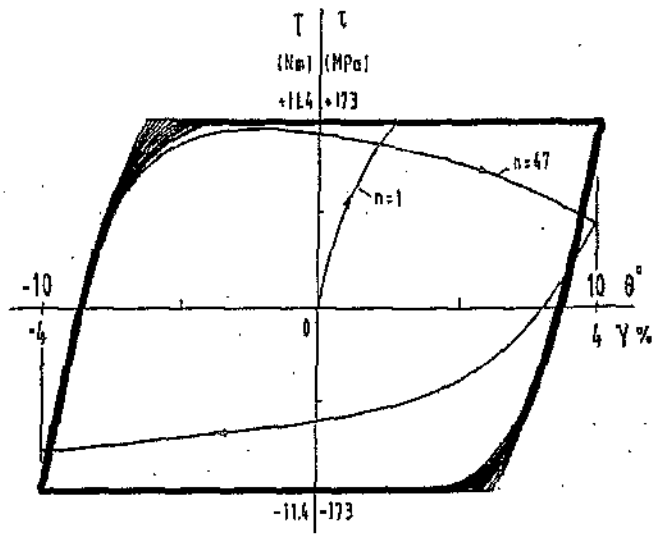

Figure 3 CC-hysteresis shown in axes of torque T versus twist θ and shear stress τ versus shear strain γ. Loop width is the inelastic strain. Material softening appears in corner rounding.

4. Analysis

Removing γ_o from each creep curve according to the scheme in Fig. 1b will enable the analysis of the testpiece creep strain γ_c to be made. Equations (6) and (7b) are applied to the twist-time recording as follows:

$$\gamma_c = C_2(\theta^\circ - \theta_o^\circ) = C_2\theta_c = a\,t^m \qquad (8)$$

It follow that if eq (8) applies to each period of creep then a double logarithmic plot between $\theta_c = (\theta^\circ - \theta_o^\circ)$ and time t, taken from the start of each reversal, would be linear. It is important to note that in these plots the creep dwell period is controlled by the strain limits. Consequently the m - value established, applies to the interval between successive reversals.

4.1 Individual Creep Curves

Figure 4 shows a selection of logarithmic plots for coupled reversals: 3 and 4, 8 and 9, 16 and 17 etc. The plots are separated for clarity by displacing the logarithmic twist scale along the vertical axis, in the manner shown for n = 2 and n = 20. Also, all gradients are shown to be positive, where, in fact, those for reversals would normally reflect the forward gradients. The initial time durations Δt (n = 2 and 3) are long, exceeding one thousand hours, failing to under 200 h in those cycles (n = 44 and 45) immediately preceding a failure. Clearly, Figure 3 shows that each creep curve conforms to eq(8) despite the successive reduction to the dwell time. Moreover, it is remarkable that despite the many reversals, the gradient $|m|$ (written, hereafter as m) for each plot remains sensibly the same, ranging from 0.51 to 0.58 with an average value m = 0.54. This m-value is in very good agreement with a previous CC study [30] at a higher temperature (600°C), a lower mean dwell stress ($\tau = \pm 160$MPa) and a lower strain range ($\gamma = \pm 3.5$ %), where dwell periods were less than 100h. These conditions revealed an average m-value of 0.55 for the forward curves and for the reversed curves m = 0.52. Variations in m would normally be attributed to the fact that m is sensitive to the subjective estimate of instantaneous strain γ_o, [22], but this has been largely avoided here from: (i) the amplification in γ_o from wind-up, as previously explained and (ii) choosing a fixed time of 10 s after each load reversal in which to read θ_o from the recordings. We conclude from this lengthy period of testing the noteworthy fact that:

Creep curves from balanced CC torsion tests are geometrically similar, with shear strain conforming to a square root-time dependence.

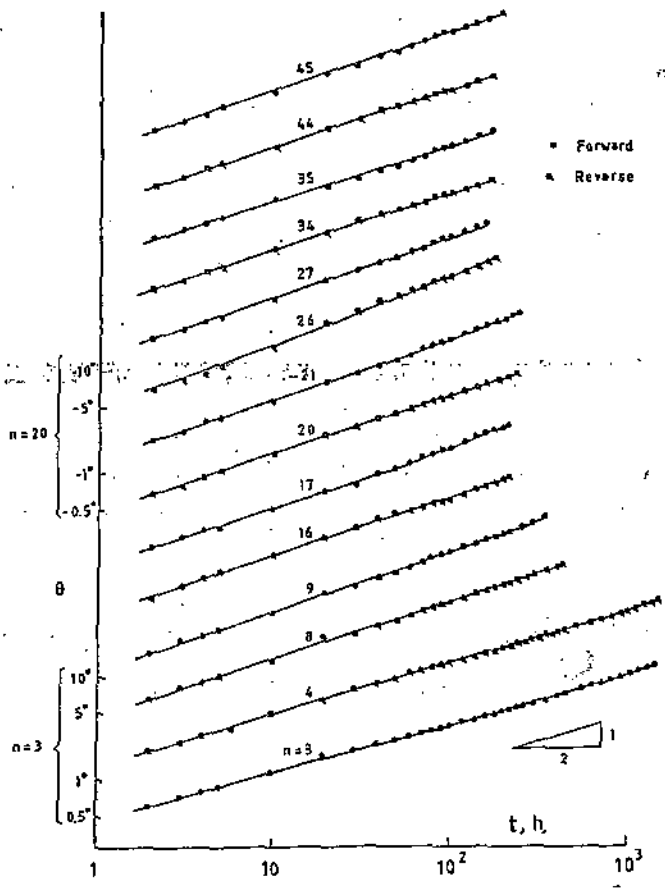

Figure 4 Application of eq(7) to creep dwell strain for a sample of adjacent cycles. Plots separated for clarity in which twist scale appears for cycles n = 3 and n = 20. Reversed dwells given positive slope to show their parallelism with forward dwells in a time dependency $\gamma_c \sim \sqrt{t}$.

The physical significance of the $\gamma_c \approx \sqrt{t}$ law for cyclic torsional creep has yet to be established though we note that an $m \approx 1/2$ value has also been reported occasionally under certain monotonic creep conditions [20-23, 34]. That the creep curves differ from each other only in size will be reflected in the coefficient a in eq (5), where a may be found at the end of each interval (see Fig. 1b), simply as:

$$a = \Delta \gamma_c / \Delta t^m = C_2 (\Delta \theta_c / \Delta t^m) \quad (9)$$

Consequently, a should depend upon cycle number n in some way until a steady state is reached, where the creep curves become identical. The logarithmic plot between a and n is shown in Fig. 5, revealing a power law dependency within the present range of data:

$$a = b\, n^q \quad (10)$$

in which the gradient of the plot gives $q = 0.45$ and $b = 0.98 \times 10^{-3}$. Thus, in combining eqs (6) and (10), we find that the cyclic shear creep strain conforms to the law:

$$\gamma_c = b\, n^q\, t^m \quad (11)$$

in which, precisely, $b = 0.98 \times 10^{-3}$, $q = 0.45$ and $m = 0.54$. Given the variability in a, when calculated from eq (9) with this average m-value, we might instead write, as a good approximation, the creep strain within each dwell period as:

$$\gamma_c = b\sqrt{(nt)} \quad (12)$$

in which $b = b(\tau)$, i.e. some function of the dwell stress to be established (most likely the cyclic equivalent of the widely accepted Norton power law for monotonic creep).

These experimentally derived relations may be used to predict the trend between Δt and n, discussed previously in Fig. 2. At the end of each dwell eq (11) is written:

$$\Delta \gamma_c = b n^q (\Delta t)^m \quad (13a)$$

so that the required relation may be written from eq (13a) as:

$$\Delta t = [(\Delta \gamma_c) / (b\, n^q)]^{1/m} = K / (n^{q/m}) = K / n^{\alpha} \quad (13b)$$

The introduction of constant K assumes that $\Delta\gamma_c$ is insensitive to cycle number n, which is observed, reasonably, when cycling between fixed strain limits. The specific relation (13b), so derived, is $\Delta t = K / n^{0.837}$ where $K = 3.5 \times 10^{-3}$. However, given that $m \approx q \approx 1/2$ in eq (12) this suggests a simple, approximate, hyperbolic relation: $\Delta t = K / n$, in which $K \approx 5 \times 10^{-3}$ when applied to Fig. 2.

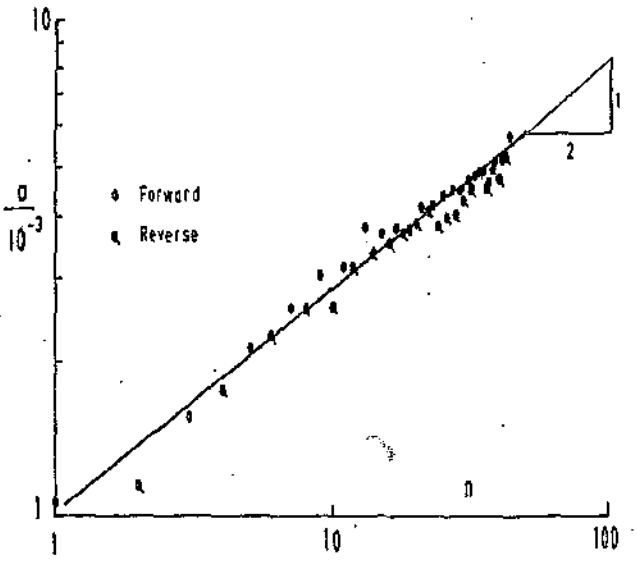

Figure 5 Dependency of coefficient a upon cycle number n, obeying an approximate relationship $a \sim \sqrt{t}$.

4.2 Bauschinger Effect

A number of authors have referred to the Bauschinger effect wherever a stress reversal occurs in creep, as reviewed by Gittus [34]. In fact, this effect refers more usually to the softening phenomenon that occurs in the plastic range where the increasing stress is suddenly reversed, i.e. the current flow stress attained from forward plasticity is reduced upon reversing the plasticity. In creep, a different interpretation of the effect is required. Here, a persistent primary creep dwell occurs, irrespective of the reversal. That the creep dwell strain will never enter the tertiary stage, implies that work hardening dominates recovery and so the material never attain the balance between these required for the steady, or minimum, creep rate that precedes the damaging tertiary stage [25]. This is because as dislocations are continually remobilised by each stress reversal they regenerate the primary creep curve repeatedly [35] with shorter duration. Thus, a progressive damage does occur under CC albeit at a lower rate than for tertiary creep. It is suggested that the reduction in dwell time (softening) for creep allies with the usual Bauschinger effect in plasticity. The analogy with time-independent plasticity becomes clearer when we observe for plasticity it is the *rate of strain hardening* that increases following a reversal in straining:

$$(d\sigma / d\varepsilon)_r > (d\sigma / d\varepsilon)_f \text{ for } \dot{\varepsilon} \Rightarrow -\dot{\varepsilon} \text{ at a given plastic } \varepsilon$$

Here an allied "softening" effect in creep, is accompanied by a continual return to a high rate of strain immediately following each reversal. That is:

$(d\sigma/dt)_r > (d\sigma/dt)_f$ for $\sigma \Rightarrow -\sigma$ following each Δt

is accompanied by a diminishing creep rate during dwell. This observation may appear misleading when, as we shall see, the strain and time accumulated from cycle to cycle *do* show the increasing (tertiary) creep rate that would be expected for simple torsional creep in this material [1]. To admit the apparently conflicting observations on creep rates, we must conclude that under CC:

Individual creep strain increments are primary in nature but they accumulate strain with time to exhaust the material's creep ductility in a tertiary manner.

4.3 Analysis of Cumulative Creep Strain

When the strain and the time at the end of each creep period are summed across all cycles (n from 1 to N) the plot between them, i.e.

$$\Sigma(\Delta\gamma_c)_n \text{ versus } \Sigma(\Delta t)_n$$

reveals an interesting feature of CC creep deformation. We see from Fig. 6, a cumulative creep curve that displays the dominant tertiary region, with its increasing rates, that have also been observed in monotonic creep tests upon this material [1]. An example of this is shown in Fig. 6 for a higher temperature (800°C), where to a magnified scale, the curve shows an inflexion between tertiary and a much smaller, initial contribution from primary creep. A description to creep curves with this feature is provided by the following form of eq (3) [10]:

$$\gamma_c = \theta_1(1 - e^{-\theta_2 t}) + \theta_3(e^{\theta_4 t} - 1)$$

For simplicity, γ_c and t have replaced the respective summations given above. The following constants: θ_1 = 0.14, $\theta_2 = 6.9 \times 10^{-4}$, θ_3 = 0.30 and $\theta_4 = 1.65 \times 10^{-4}$ provide a reasonable fit to the cumulative creep curve shown. Also shown in Fig. 6 are the cumulative plots for two further CC tests conducted under different conditions [30]. These reveal that for reversed torsional creep, it is the cumulative time and not the cumulative strain which provides a more sensitive criterion of fracture to the changed conditions. The fact that cumulative strain is more nearly constant lies with the fact that a continual reversal of the shear strain prevents it from attaining the critical value for torsional buckling. While this can be said for a ductile stainless steel it would not be true to draw a similar conclusion for a limited ductility, cavity forming, nimonic alloy that fails by shear under torsional creep before it buckles [32]. Examples of the mode of failure in each material are shown in Figs 7a,b. The monotonic torsional-buckling mode in the steel limits the range of uniform shear strain to a mere 20 % (see Fig.7a) in spite of

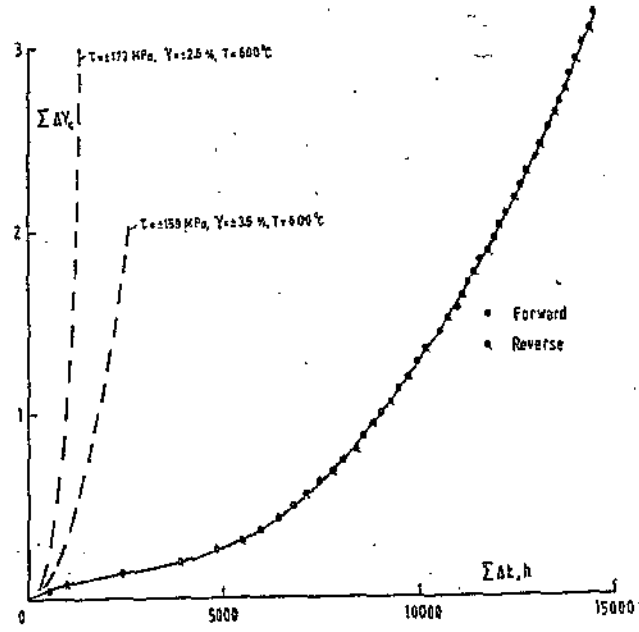

Figure 6 Cumulative plot between strain and time from all periods of CC dwell, showing the re-appearance of a dominant tertiary region that is a feature of a simple torsional creep curve (lower curve) for this material. Additional plots [31] for an austenitic stainless steel 800H under CC suggest that accumulated time, not strain, would provide the more sensitive measure for life predictions embodying dwell stress and temperature.

the large angular rotations attained. In contrast, a lesser amount of strain to failure is accommodated by cavity growth in the nickel-base alloy (see Fig. 7b).

5. Life Prediction

Figure 6 shows that the cumulative ductility for this material in an impressive $\gamma_f = \Sigma\Delta\gamma_c = 3.1$, which is far greater than the monotonic creep strain under a similar stress and temperature [1]. The problem in using monotonic creep data is one of tubular buckling limiting the shear strain to ≈ 0.3, so making its "rupture" strain less than that for cyclic creep by one order. Normally, one seeks to identify γ_f with the appropriate tensile creep ductility ε_f particularly where, for stainless steel, much creep rupture exists [36 - 38], but this raises the debatable issue of whether an equivalence criterion exists between γ_f and ε_f. Alternatively, and more appropriately, the CC test itself could be used to supply the baseline shear strain at fracture γ_f so that the cyclic life prediction amounts to a simple division by the incremental dwell strain, i.e. $N = \gamma_f/\Delta\gamma_c$. The partitioning implied by this division suggests a strain-based method for predicting cyclic life, though as we have seen, γ_f may be too insensitive a

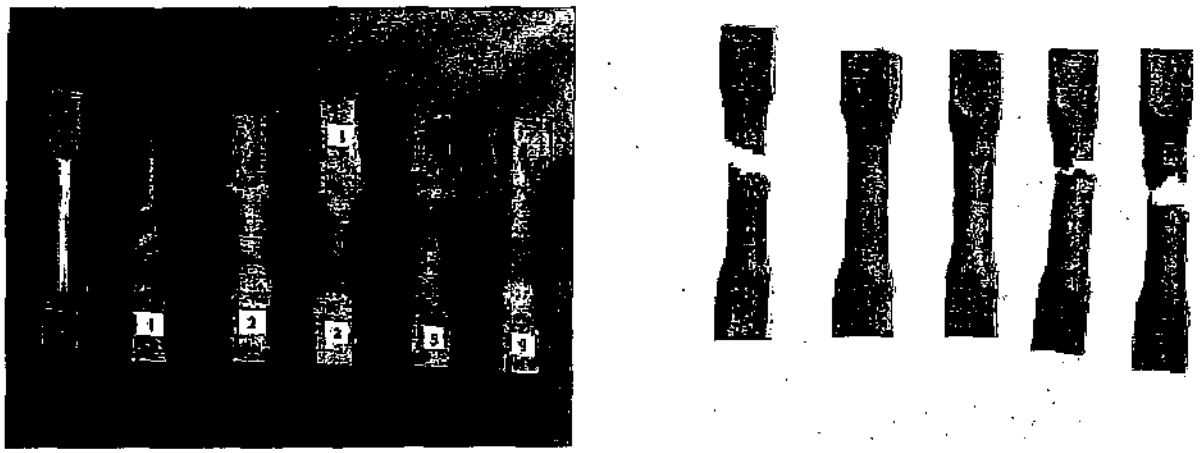

Figure 7 (a) Monotonic torsional buckling failures in a stainless (800H) and (b) CC shear failures in a nimonic alloy (IN 597)

measure to the CC test conditions here. Consequently, a time-based prediction may be preferred. In Fig. 6, the cumulative time to rupture, $\Sigma\Delta t \approx 15 \times 10^3$ h, would be expected to exceed the monotonic rupture time for a simple torsion test by a far lesser ratio than the ratio between their corresponding rupture strains. These ratios between the fracture strains and times from each type of test are employed in the following schemes for a life prediction.

5.1 Strain Fraction

This form of eq (5) separates the three test variables: cycle time and cycle number from the dwell stress in manner amenable to a life prediction. Thus, if the latter is to be based upon an exhaustion of a material's monotonic creep ductility γ_f at the given peak stress τ and temperature, we may write:

$$b(\tau)\Sigma\sqrt{(n\,\Delta t_n)} = D\,\gamma_f \qquad (14)$$

for a summation $n = 1$ to N, where D is a constant that may be taken differently from unity to reflect the character of the limiting ductility (strain accumulated at fracture) under steady and cyclic stress conditions. For example, $D > 1$ if each reversal serves to repair partially the damage arising from its preceding neighbour, as with cracks/voids being continually opened and closed in directions at ± 45° directions to the testpiece axis when such damage arises under a principal tension. With this partial healing from each reversal, the cumulative damage proceeds at a slower rate than under a steady application of stress, so raising the fracture strain and prolonging life. Here we would expect Fig. 6 to have extended both the strain and the time axes compared to a monotonic creep curve [1] where, the shorter creep life arises from the dominant tertiary stage in stainless steels.

Thus, substituting the relation between Δt_n and n from eq (13b) into eq (14), after having made the summation, leads to

$$b\sqrt{[K\,(1 + 2^{1-\alpha} + 3^{1-\alpha} + \ldots + N^{1-\alpha})]} = D\gamma_f \qquad (15a)$$

from which N can be found. For example, if we substitute instead, the simple hyperbolic relation $\Delta t_n = K/n$, eq (15a) allows for $\alpha = 1$, giving N directly as:

$$N = (1/K)\,(D\gamma_f / b)^2 \qquad (15b)$$

5.2 Time Fraction

Alternatively, applying the time fraction rule (4) to connect the two tests, gives:

$$\Sigma\Delta t_n = L\,t_f \qquad (16a)$$

for a summation from $n = 1$ to N, where L is a constant, reflecting the difference in their lives (the accumulated time to fracture). Using $\Delta t_n = K/n$, for simplicity, allows the cyclic life to be found from:

$$\Sigma\,(1/n) = L\,t_f / K \qquad (16b)$$

for a summation from $n = 1$ to N. No theoretical advantage is offered by adopting one fractional method over the other to predict life, i.e. we may partition the curve in strain or time appropriate to our choice of fraction. A geometrical interpretation of this type of approach rests with having the appropriate monotonic creep curve available and overlaying upon it the strain and time accumulated from each period of dwell (as in Fig. 6), so that the co-ordinates at fracture establish either D or L as required. However, if low cycle fatigue (LCF) plays an interactive role, then it is more usual to combine a cycle fraction from fatigue with the time fraction from creep in the linear form of Taira's eq (4). There was

some evidence of LCF under the present test conditions, namely, a fast plastic strain did appear within the slight rounding of the more advanced hysteresis loops in Fig. 3. However, because creep has been the major contributor to the inelastic strain range in every cycle, the partitioning of that range into the creep and plastic components would be inexpedient under these test conditions.

6. Concluding Remarks

Under, cyclic torsional creep of a stainless steel, the Bauschinger effect is manifested in raising the creep rate with each reversal so that creep during a strain-limited dwell is always primary in character. The shear creep strain at any given time t within a given dwell cycle n follows a square root law $\gamma_c \sim \sqrt{(nt)}$ in both the forward and reversed directions. The diminishing creep dwell period is approximately inversely proportional to the cycle number. In contrast to the individual dwell periods of primary creep, a tertiary behaviour applies to the strain and time accumulated from successive dwells, reminiscent of the tertiary creep curve found from a monotonic creep test upon this material. Such observations facilitate the prediction of cyclic creep life from the monotonic test using, either the ratio between their rupture strains, or their rupture times. The latter provides the more sensitive criterion, given there is little creep-fatigue interaction for a CC test with extended dwell periods.

The physical significance of the "root time law" is believed to be a manifestation of the Bauschinger effect, where each reversal remobilises dislocations to raise the creep rate. Power time laws t^m for creep are generally associated with work hardening arising from an increasing dislocation density. One particular, theoretical basis for the a $t^{1/3}$, often found in primary monotonic creep, has been based upon this mechanism of hardening [39]. In balanced, strain-limited CC, however, the dislocation density cannot increase beyond a certain limit by the action of the repeated reversals that continually impose the Bauschinger effect upon the structure. Consequently, it is believed that the $t^{1/2}$ law revealed here will express the time-dependence of the strain-limited, balanced, cyclic creep test for many metals and alloys. Its counterpart, the $t^{1/3}$ law, has long been understood to express time-dependence of similar materials under monotonic creep conditions.

References

1. Rees, D. W. A. *Int Jl Press and Piping*, 1985, **20**, 101.
2. Cottrell, A. H. *Jl Mech Phy Solids*, 1952, **1**, 53.
3. Conway, J. B. *Numerical Methods for Creep and Rupture Analysis*, Gordon and Breech, 1969.
4. McVetty, P. G. *Mech Eng*, 1934, **56**, 149.
5. Garofalo, F. *Fundamentals of Creep and Creep Rupture in Metals*, Macmillan 1965.
6. Andrade, E. N. da C. and Aboav, D. A. *Proc. Roy. Soc.* 1964, **203A**, 352.
7. Evans, W. J. and Wilshire, B. *Met Trans*, 1970, **1**, 2133.
8. Davies, P. W., Evans, W. J. , Williams, K. R. and Wilshire, B. *Scripta Met*, 1969, **3**, 671-674.
9. Evans, R. W, Parker, J. D, and Wilshire, B. *Recent Advances in Creep and Fracture of Engineering Materials and Structures*, Pineridge Press, 1982.
10. Evans, R. W. and Wilshire, B. *Introduction to Creep*, Inst of Mats, 1993.
11. Halford, G. R., Hirshberg, M. H. and Manson, S. S. *ASTM, STP*, 1973, **520**, 658.
12. Spera, D. A. *NASA Rpt* 1969, TND-5489.
13. Taira, S. *Creep in Structures* (Ed Hoff, N.) Academic Press, New York, 1962, 96.
14. Polhemus, J. F, Spaeth, C. E. and Vogel, W. H. *ASTM, STP*, 1973, **520**, 625.
15. Nutting, P. G. *Proc ASTM*, 1921, **21**, 1162.
16. Andrade, E. N. da C. *Proc. Roy. Soc.* London, 1910, **A84**, 1; 1914, **A81**, 1.
17. Graham, A. and Walles, K. F. A. *Aero Res Cl*, CP680, 1963, HMSO, London.
18. Wyatt, O. H. *Proc Phys Soc*, 1953, **66B**, 459.
19. Olds, G. C. E. *Proc Phys Soc*, 1954, **67B**, 832.
20. Kennedy, A. J. *Brit Jl Appl Phys*, 1953, **4**, 225.
21. Crussard, C. *Revue de Metallurgie*, 1946, **43**, 307.
22. Crussard, C. *Proc Jnt Int Conf on Creep*, I Mech.E/ASTM/ ASME, 1963 (Book 2), Paper 75, 2-123.
23. Bhattacharya, S, Congreve, W. K. A. and Thompson, F. C. *Jl Inst Metals*, 1952-3, **81**, 83.
24. Rees, D. W. A. *Proc Roy Irish Acad*, 1981, **81** (A), No.2, 167.
25. Lagneborg, R. *Int Met Rev*, 1972, **17**, 130.
26. Kitagawa, M., Jaske, C. E. and Morrow, J. *ASTM, STP*, 459, 100.
27. Murakami, S. and Ohno, N. *Int Jl Sol & Struct*, 1982, **18**, 597.
28. Hayhurst, D. R, Trampczynski, W. A, and Leckie, F. A. *Acta Met*, 1980, **28**, 1171.
29. Morris, D. G. and Harris, D. R. *Jl Mat Sci*, 1978, **13**, 985.
30. Rees, D. W. A. *Proc 3rd Int Cong on Thermal Stress*, (Eds Skrzypek, J. J. and Hetnarski, R. B.) Cracow, Poland, 1999, 219.
31. Rees, D. W. A. Proc Euromat 2000: *Advances in Mechanical Behaviour, Plasticity and Damage*, (Eds Miannay, D. et al) Tours, France, 2000, **2**, 1315.
32. Rees, D. W. A. and Dyson, B. *Int Jl Plasticity*, 1986, **2**, 1.
33. Ericksen, R. H. and Jones, G. J. *Met Trans ASM*, 1972, **3**, 1735.
34. Gittus, J. *Creep*, Viscoelasticity and Creep Fracture in Solids, Applied Science, 1975.
35. Gittus, J. *Phil Mag*, 1971, **24**, 1423.
36. Hoyt, S. L. Metal Data, Ch. 7, Reinhold, New York, 1952.
37. Blackburn, L. D. Proc: *The Generation of Isochronous Stress-Strain Curves*, (Ed. Schaefer, A.O.) *ASME*, Nov. 1972, p.15.
38. Guest, J. C. Proc: *A Status Review of Alloy 800* (Ed. Pugh, S. F), Brit. Nuclear Energy Soc, 1974, 251.
39. Howe, P. W. H. *Theoretical basis of power laws of creep*, NGTE Rpt. S.4496, Jan. 1967.